

## **Geometric and material non-linear wave propagation with the material point method**

Bruno Zuada Coelho<sup>1,\*</sup>, Alexander Chmelnizkij<sup>2</sup>, Jürgen Grabe<sup>2</sup>

<sup>1</sup>Geo-engineering, Deltares, Delft, The Netherlands

<sup>2</sup>Institute of Geotechnical Engineering and Construction Management, Hamburg University of Technology, Hamburg, Germany

\* E-mail: Bruno.ZuadaCoelho@deltares.nl

### **ABSTRACT**

This paper presents the numerical modelling of one-dimensional wave propagation with the material point method, considering geometric and material non-linearity. Geometrical non-linearity corresponds to the non-linear relation between strain and displacements due to large deformations, whilst material non-linearity is caused by the non-linear relation between stress and strain. In this study, a finite solid column will be used as an example to illustrate the effect of both non-linearities in the overall response.

**KEY WORDS:** Material point method; wave propagation; non-linear analysis

### **INTRODUCTION**

The modelling of large deformations and dynamic problems is of great importance for geomechanical problems. Although these topics have been the subject of extensive research on its own, the modelling of problems such as earthquakes, impact loads and explosions are still challenging, as they involve the combination of large deformation analysis, with dynamic loading and non-linear material behaviour.

The recent developments in mesh-free methods have allowed exploring the large deformation behaviour. Among these methods, the material point method (MPM) has been developed and applied successfully to several geomechanical problems (e.g. Phuong et al. 2016, Soga et al. 2016). In the material point method the continuum material is represented by a set of Lagrangian points (material points) that move through an Eulerian background mesh. The material points contain all the properties of the continuum, such as mass, stress, strain and material parameters. Therefore, the material point method can be seen as a combination of both Lagrangian and Eulerian formulations. The problems related to mesh distortion under large deformations are circumvented, as well as the diffusion associated with the convective terms of the Eulerian approach (Sulsky et al. 1994, Sulsky et al. 1995). The use of Lagrangian material points conserves mass and allows the use of complex history dependent stress-strain material models. The hypoplasticity is a usual non-linear and inelastic constitutive model which is used to simulate the behavior of sand (Gudehus 1996, von Wolffersdorf 1996).

This paper presents a study of the effect of geometric and material non-linearities on the one dimensional wave propagation through a solid column. The objective is to illustrate the importance of the two sources of non-linearities on the response of a well-defined problem.

### **NON-LINEAR GEOMETRIC ANALYSIS**

The effect of non-linear geometry on the wave propagation has been evaluated by computing the one dimensional wave propagation travelling through an elastic dry solid material. Figure 1 presents the geometry of the problem. The solid column has a finite length  $L$ , and it is submitted to a compressive load  $p_0$ , suddenly applied at the top ( $x = L$ ). At the bottom ( $x = 0$ ) the column is assumed to be fixed. The column has a constant cross section  $A$ , a Young's modulus  $E$ , Poisson ratio  $\nu$  and density  $\rho$ . Within the low strain regime, the solution of the equation of motion can be found as a Fourier expansion (Churchill, 1972):

$$\begin{aligned}
 u &= \frac{p_0}{K} \left[ x + \frac{8L}{\pi^2} \sum_{n=1}^{\infty} \frac{(-1)^n}{(2n-1)^2} \sin(\lambda x) \cos(\lambda ct) \right] \\
 p &= \frac{p_0}{K} \left[ 1 + \frac{8L}{\pi^2} \sum_{n=1}^{\infty} \frac{(-1)^n}{(2n-1)^2} \cos(\lambda x) \cos(\lambda ct) \right]
 \end{aligned}
 \tag{1}$$

where  $u$  and  $p$  are, respectively, the displacement and stress, which are function of the wave velocity of the solid  $c = \sqrt{K/\rho}$ , and the solid bulk modulus  $K$ :

$$K = \frac{E(1-\nu)}{(1+\nu)(1-2\nu)}.
 \tag{2}$$

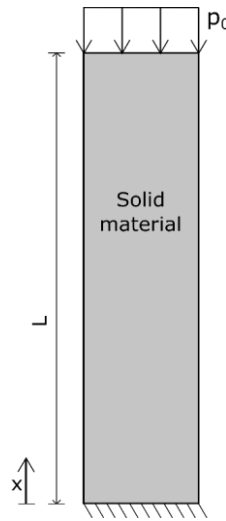


Figure 1 Overview of the solid geometry and loading conditions

The numerical analyses are conducted with the MPM software Anura3D (2018). The solid column is modelled as a 1 m column with an element size of 0.01 m. Low-order tetrahedral elements with 4 material points per element are used. A structured mesh is used in the analyses. The load is applied on the nodes at the top of the solid column. The nodes at the bottom of the column are fixed in vertical direction. The solid is modelled as a linear elastic material with the parameters given in Table 1.

**Table 1 Material parameters for the solid column**

Material parameter	Value
Density soil [kg/m <sup>3</sup> ]	2600
Porosity [-]	0.2
Young modulus [kPa]	5000
Poisson ratio [-]	0.3

Figure 2 shows the displacement and stress for a material point located at  $0.5 L$ , for two different scenarios:

- small deformation:  $p_0 = 1 \text{ kN/m}^2$ ;
- large deformation:  $p_0 = 10 \text{ kN/m}^2$ .

The analytical solution is also available, and has been computed with  $n = 100$  terms for the Fourier series. All the results are normalised for the sake of comparison. For the small deformation analysis ( $p_0 = 1 \text{ kN/m}^2$ ) there is an agreement between the numerical and analytical results. A clear propagation of the compression wave is identified. The wave starts travelling at  $t = 0$  until it reaches the bottom boundary where it is reflected, creating a tension wave travelling in the opposite direction. As there is no damping in the system, the wave keeps on travelling through the solid column indefinitely. The time required for the wave to travel along the solid column is correctly

captured as well as the average amplitude of the displacement and stress. In the numerical analysis, the maximum and minimum values of the stress are not constant (Figure 2 b), as in the analytical solution, but oscillate around the exact value. This oscillation is related to the numerical discretisation and the integration of the equations of motion (Idesman *et al.* 2011).

When the load is increased ( $p_0 = 10 \text{ kN/m}^2$ ), the displacement and stress of the material point differ from the analytical solution. Immediately after the load application the response is the same for both analyses (up to  $t = 1.5$ , Figure 2 a). However, as the load reaches the end of the column, the pattern of the wave propagation becomes different for the large deformation analysis. This is because the length of the column is significantly reduced, when the load is  $p_0 = 10 \text{ kN/m}^2$ , which causes the reduction of the travelling time. When the load is  $p_0 = 1 \text{ kN/m}^2$ , the column deformation is small, therefore this effect is negligible. In the large deformation analysis, a smoothing of the solution occurs. The same differences are identified for the stress (Figure 2 b). After the initial reflection at the bottom of the column, the stress pattern differs for the large deformation analysis.

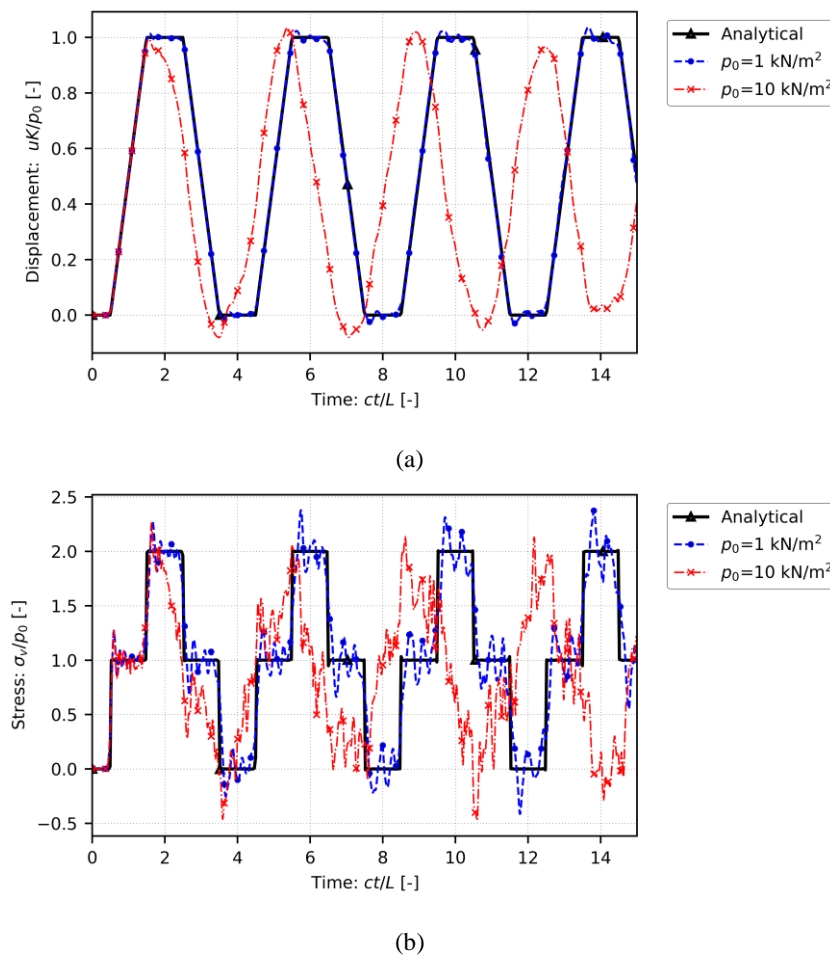
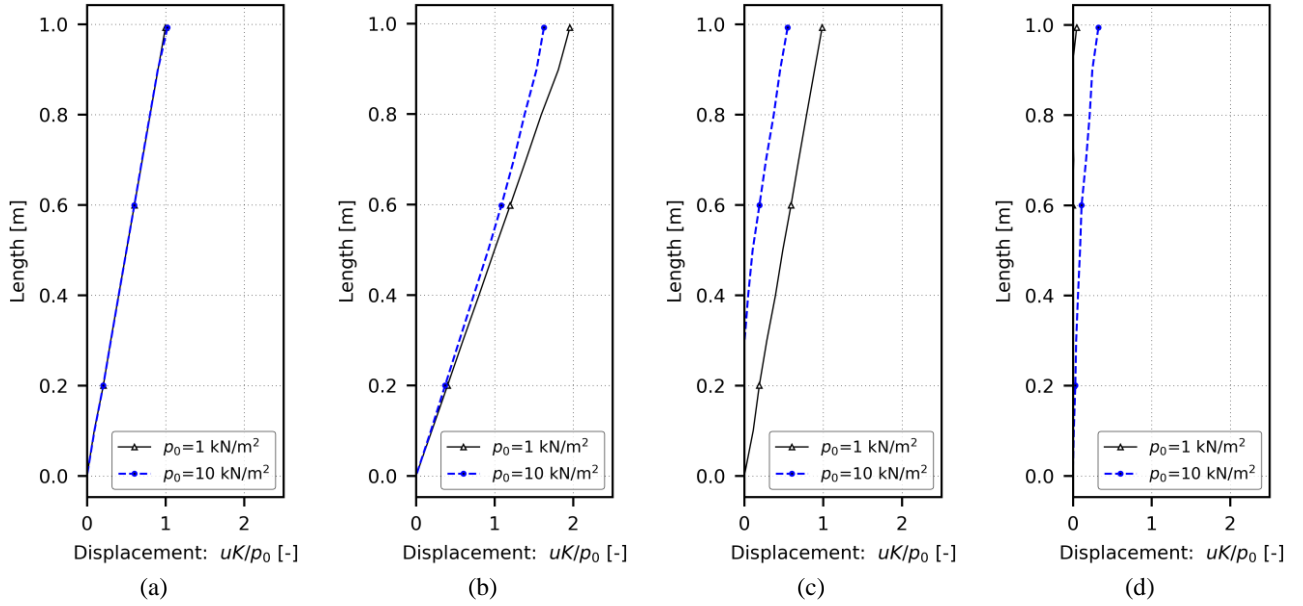


Figure 2 Comparison of the velocity for a point located on the solid column: (a) displacement and (b) stress of a point located at  $x = 0.5 L$ .

Figure 3 shows the displacement profile of the column at different times, for both small and large deformation analysis. The figure presents the results at  $t = 1, 2, 3$  and  $4$ , which correspond to the time at which the wave reaches the bottom and top boundaries (according to the small deformation solution). As expected, at  $t = 1$  both analysis give the same results (Figure 3a). The differences arise after the initial reflection of the wave at the bottom of the column. When the wave reaches the top boundary at  $t = 2$  (Figure 3b) the displacement amplitude is smaller for the large deformation analysis, because at  $t = 2$  the wave has already reflected for the large deformation analysis (due to the length reduction as previously explained). The differences between small and large deformation analysis tend to increase with time, as the travelling distance remains smaller for the large deformation analysis (Figure 3c-d).


 Figure 3 Displacements for the column at different normalised times: (a)  $t = 1$  (b)  $t = 2$  (c)  $t = 3$  and (d)  $t = 4$ .

## NON-LINEAR MATERIAL ANALYSIS

Material behaviour determines the shape of a propagating wave and its evolution in time. Linear elastic models lead to a preserved shape corresponding to the initial or boundary condition. In non-linear materials the propagation velocity of waves in general is a function of different state variables and therefore not constant. This section compares the propagation of continuous and discontinuous boundary conditions with two different material models. Our reference material model is the linear elastic, where the propagation speed is constant. In contrast to the linear elastic model the hypoplastic model (Gudehus 1996, von Wolfersdorf 1996) depends on the current state of the material. Although different models were published within the hypoplastic theory, the focus will be on the model presented by Niemunis (1997). The hypoplastic material parameters were obtained from Grabe et al. (2014). The linear elastic and hypoplastic soil parameters used in the calculations are shown in Table 2.

**Table 2 Material parameters used in the linear elastic and hypoplastic analysis**

Material parameter	Value
Density soil [kg/m <sup>3</sup> ]	2650
Porosity [-]	0.4
Linear Elasticity	
Young modulus [kPa]	2000
Poisson ratio [-]	0.1057
Hypoplasticity	
$\varphi_c$ critical state friction angle [°]	30
$h_s$ granular hardness [kN/m <sup>2</sup> ]	5.8e+6
$n$ exponent [-]	0.28
$e_{d0}$ minimum void ratio [-]	0.53
$e_{i0}$ critical void ratio [-]	0.84
$e_{c0}$ maximum void ratio [-]	1.00
$\alpha$ exponent [-]	0.13
$\beta$ exponent [-]	1.05
$R$ maximum value of inter-granular strain [-]	0.0001
$m_R$ stiffness ration at a change of load direction of 180 [-]	2.0
$m_T$ stiffness ration at a change of load direction of 90° [-]	5.0
$\beta_R$ exponent [-]	0.5
$\chi$ exponent [-]	6.0
$K_s$ bulk modulus solid [kN/m <sup>2</sup> ]	3.7e7

The hypoplastic model is non-linear in the compressing and unloading case. This study will be restricted only to the compressing scenario. Consider a column as shown in Figure 1 of a length  $L=5\text{m}$ , with the time-dependent loading function  $p_0(t)$  shown in Figure 4. The first meter of the column is discretised by elements of the length 1 mm. After the first meter the element size increases up to a length of 30 mm. This is done to investigate the mesh-dependency of the solution and to reduce the calculation time. The numerical analyses have been performed with Anura3D (2018).

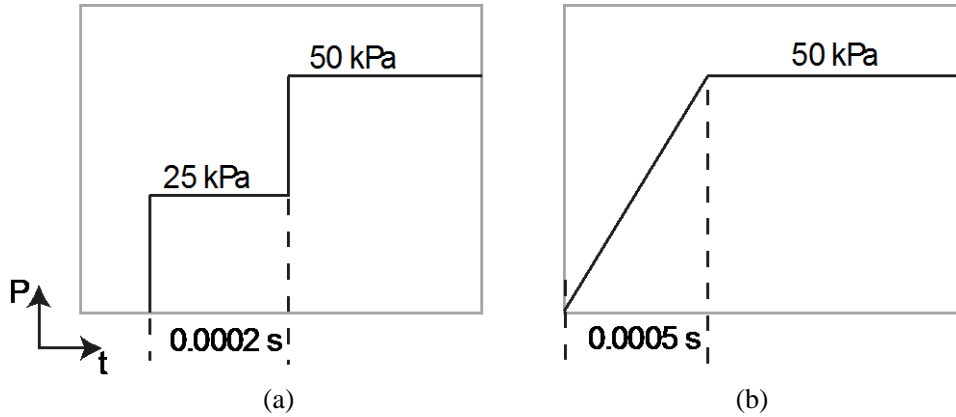


Figure 4 Load functions: (a) stepwise and (b) linear load functions

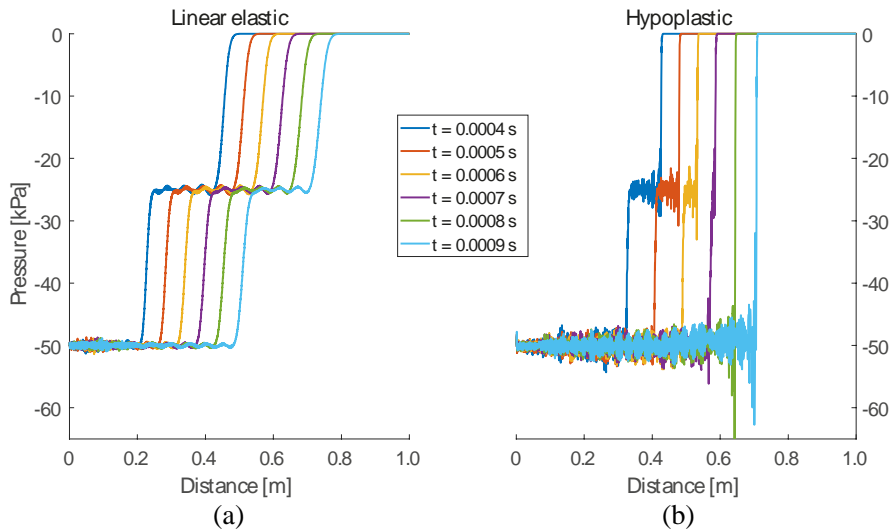


Figure 5 Solutions for stepwise loading with: (a) linear elastic and (b) hypoplastic material model

The stepwise load function is discontinuous with two pressure levels, one at 25 kPa and the second at 50 kPa. As discontinuities in an explicit Forward Euler solution will lead to large oscillations, bulk viscosity (van Neumann & Richtmyer 1950) with  $c_L = 0.2$  and  $c_Q = 1.2$  is applied. In Figure 5 the results for the linear elastic and hypoplastic material model are shown for the stepwise loading conditions. In the case of linear elasticity both pressure jumps are propagating with a constant velocity. The application of bulk viscosity smoothens the solution, therefore the discontinuous character of the analytical solution is missing. In the hypoplastic solution the second pressure jump is propagating faster due to a higher stress state in the material. After 0.0008 s the second jump catches up the first one and the wave propagates as one jump of the magnitude of 50 kPa. This observation indicates one of the main aspects of non-linear material behaviour. In the case of hypoplasticity the propagation speed increases with higher stresses. Therefore discontinuities can occur in a solution even if the boundary conditions are continuous.

In Figure 6 shows the results for the linear load function. While the linear elastic case preserves the shape of the loading function the hypoplastic solution loses continuity already after few calculation steps. The increasing pressure at the boundary leads to an increasing propagation speed. Therefore a discontinuity forms in which mounts up during the calculation. To reduce the oscillations bulk viscosity with  $c_L = 0.42$  and  $c_Q = 1.2$  is applied.

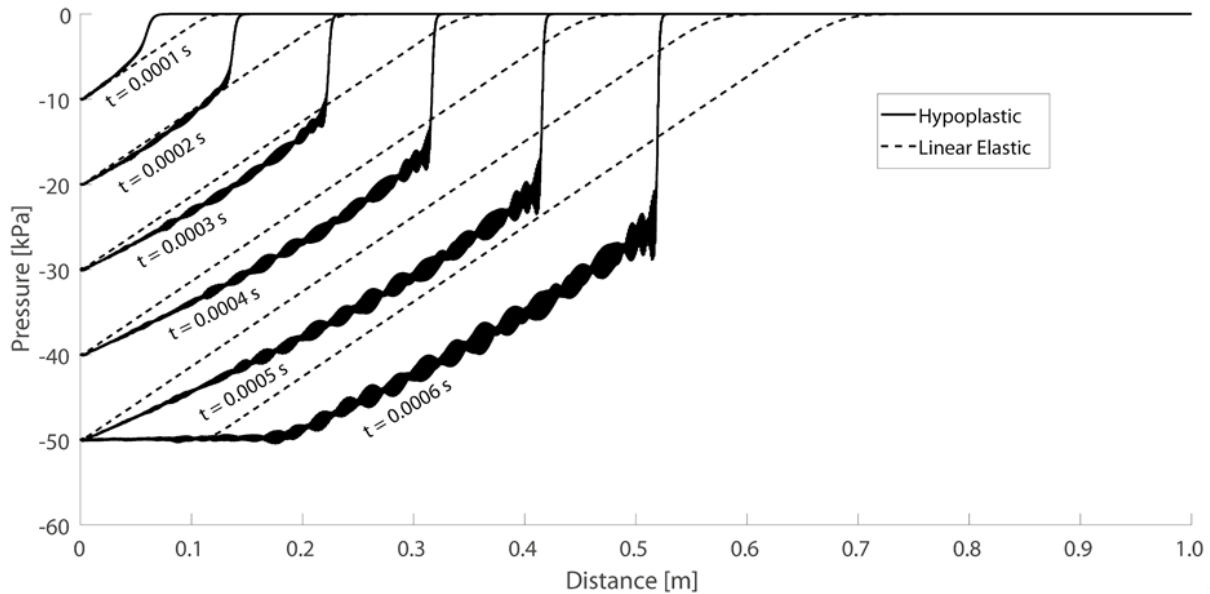


Figure 6 Linear elastic and hypoplastic solutions for linear loading.

In contrast to the linear elastic the hypoplastic solution tends to oscillate. These oscillations are growing as the magnitude of the jump is increasing even though bulk viscosity is applied. Once the 50 kPa pressure level reaches the jump the wave propagates as a single discontinuity of the magnitude of 50 kPa like in the stepwise loading case.

## CONCLUSIONS

This paper presents the effect of geometric and material non-linearities on the one-dimensional wave propagation problem.

The geometric non-linearity was found to influence the wave propagation pattern on the one-dimensional column. When the deformation of the column becomes significant, the time that requires the wave to travel along the column is reduced, causing a change in the propagation pattern and the smoothing of the response.

The effect of material non-linearity was illustrated by comparing the elastic and hypoplastic material models. In the numerical simulations linear time integration schemes were applied to solve the non-linear problem. It was shown that the elastic material model preserves the loading discontinuities, while the same does not apply for the hypoplasticity material model. The application of bulk viscosity smoothens the discontinuities, preventing large oscillations of the solution.

All the results presented in this paper regard a simple problem (one-dimensional solid column). For problems involving more complicated geometries, the effects of non-linearities are likely more complex, and harder to distinguish.

## REFERENCES

- Anura3D (2018). *Anura3D MPM software v.2018.1*. Anura3D MPM Research Community, Delft, the Netherlands.
- Niemunis A & Herle I. (1997). Hypoplastic model for cohesionless soils with elastic strain range. *Mechanics of Cohesive-frictional Materials: An International Journal on Experiments, Modelling and Computation of Material and Structures*, 2(4): 279–299.
- Churchill RV. (1972). *Operational Mathematics, 1rd edn*. McGraw-Hill, New York, US.
- Grabe J, Hamann T & Chmelniczki A. (2014) Numerical simulation of wave propagation in fully saturated soil modelled as a two-phase material. *Eurodyn 2014 9th International Conference on Structural Dynamics*, Porto, Portugal, pp. 631-637.
- Gudehus G. (1996), A comprehensive constitutive equation for granular materials. *Soils and Foundations* 36(1): 1-12.

- Phuong NTV, Van Tol AF, Elkadi ASK & Rohe A. (2016). Numerical investigation of pile installation effects in sand using material point method. *Computers and Geotechnics* 73: 58–71.
- Idesman AV, Schmidt M, & Foley, JR. (2011). Accurate finite element modeling of linear elastodynamics problems with the reduced dispersion error. *Computational Mechanics*, 47(5): 555-572.
- Soga K, Alonso E, Yerro A, Kumar K & Bandara S (2016). Trends in large-deformation analysis of landslide mass movements with particular emphasis on the material point method. *Géotechnique* 66(3): 248–273.
- Sulsky, D., Chen Z, & Schreyer HL (1994). A particle method for history-dependent materials. *Computer Methods in Applied Mechanics and Engineering*. 118(1): 179–196.
- Sulsky D, Zhou S-J, & Schreyer HL (1995). Application of a particle-in-cell method to solid mechanics. *Computer Physics Communications*. 87(1): 236–252.
- Von Neumann, J. & Richtmyer, R. D. (1950) A Method for the Numerical Calculation of Hydrodynamic Shocks. *Journal of Applied Physics*, 21(3): 232–237.
- von Wolffersdorff P.-A. (1996), A hypoplastic relation for granular materials with a predefined limit state surface. *Mechanics of Cohesive-frictional Materials*, 1: 251–271.